Role of the composition of humic substances formed during thermal hydrolysis process on struvite precipitation in reject water from anaerobic digestion

Pavez-Jara, Javier; Iswarani, Widya P.; van Lier, Jules B.; de Kreuk, Merle K.

DOI
10.1016/j.jwpe.2024.104932

Publication date
2024

Document Version
Final published version

Published in
Journal of Water Process Engineering

Citation (APA)
Pavez-Jara, J., Iswarani, W. P., van Lier, J. B., & de Kreuk, M. K. (2024). Role of the composition of humic substances formed during thermal hydrolysis process on struvite precipitation in reject water from anaerobic digestion. *Journal of Water Process Engineering*, *59*, Article 104932. https://doi.org/10.1016/j.jwpe.2024.104932

Journal of Water Process Engineering 59 (2024) 104932

Contents lists available at ScienceDirect

Journal of Water Process Engineering

journal homepage: www.elsevier.com/locate/jwpe

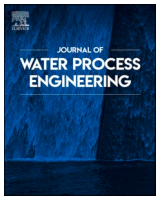

Role of the composition of humic substances formed during thermal hydrolysis process on struvite precipitation in reject water from anaerobic digestion

Javier Pavez-Jara [a,*], Widya P. Iswarani [a,b,1], Jules B. van Lier [a], Merle K. de Kreuk [a]

[a] Department of Water Management, Delft University of Technology, Building 23 Stevinweg 1, 2628 Delft, the Netherlands
[b] Wetsus, European Centre of Excellence for Sustainable Water, Oostergoweg 9, 8911, MA, Leeuwarden, the Netherlands

ARTICLE INFO

Editor: Sadao Araki

Keywords:
Struvite
Phosphate recovery
Melanoidins
Humic acid
Thermal hydrolysis process

ABSTRACT

Thermal hydrolysis process (THP) is a widely used pre-treatment method in the anaerobic digestion (AD) of waste municipal sewage sludge. A post AD dewatering step of the digestate produces a liquid stream called reject water. THP increases the concentration of humic substances (HSs) and nutrients in the produced reject water. Struvite precipitation is a widely used technique to remove and (potentially) recover PO_4^{3-}-P and the corresponding amount of total ammoniacal nitrogen from reject water. The chemical characteristics of the THP-produced HSs influence reaction yields and morphology of struvite. In our current study, struvite batch precipitation experiments were conducted at different pHs, and different concentrations of HSs, consisting of either melanoidins or humic acids. Our results showed that at pH 6.5 struvite precipitation was severely retarded. However, increased concentrations of melanoidins at pH 6.5 enhanced struvite precipitation. Batch experiments conducted at pH 7.25 and 8 with increased melanoidins concentrations showed PO_4^{3-}-P precipitation yields over 86 %. Humic acids negatively impacted struvite precipitation at all analysed pH values, presumably because of Mg^{2+} complexation. Morphological analysis showed that the presence of both HSs affected Feret diameters, aspect ratio, and cleavage pattern of struvite. Also, HSs rendered coloured crystals. Overall, our results showed that struvite precipitation is affected by HSs intrinsic characteristics, affecting yield, morphology, and colour of the formed precipitates.

1. Introduction

Pre-treatment technologies for waste municipal sewage sludge prior to anaerobic digestion (AD) in wastewater treatment plants (WWTPs) are implemented to enhance energy efficiency, reduce costs and residues, and sanitize AD digestates [1,2]. The thermal hydrolysis process (THP) is widely used in full-scale AD pre-treatments installations [3], using different configurations such as SUSTEC® (Netherlands), CAMBI® (CAMBI, Norway), Lysotherm® (Eliquo Technologies, Germany), Exelys™, and Bio Thelis™ (Veolia, France). In all mentioned THP technologies, primary sludge, waste activated sludge, or a combination of both are exposed to elevated temperatures (160-180 °C) for a defined period of time to enhance the anaerobic digestibility and digestate dewaterability, to reduce pathogen concentrations, and to shorten the AD solids retention time [4,5]. Nonetheless, the use of high temperatures during THP alters the chemical composition of the sludge matrixes, producing a particular type of humic substances (HSs) known as melanoidins via the Maillard reaction [6].

Melanoidins are coloured compounds, consisting of polymerised aromatic groups, and result from a series of reactions between reducing sugars and amino groups present in proteins [7,8]. The Maillard reaction already occurs at room temperature, but is pronounced at higher temperatures [9] such as those occurring during THP. Melanoidins can be classified based on their pH-dependent solubility as a result of their variable isoelectric point in the same way as HSs [10]. The pH-dependent solubility of melanoidins allows us to classify them, like HSs, as fulvic acids, humic acids, and humins [11]. In addition, melanoidins behave as polydentate ligands, complexing cations in solution,

* Corresponding author.
E-mail addresses: j.a.pavezjara@tudelft.nl (J. Pavez-Jara), widya.iswarani@wetsus.nl (W.P. Iswarani), j.b.vanLier@tudelft.nl (J.B. van Lier), m.k.dekreuk@tudelft.nl (M.K. de Kreuk).
[1] Present address.

https://doi.org/10.1016/j.jwpe.2024.104932
Received 7 November 2023; Received in revised form 4 January 2024; Accepted 28 January 2024
Available online 10 February 2024

due to the presence of negatively charged ketone and hydroxyl groups in their structure [12,13]. Also, under AD conditions melanoidins may behave as recalcitrant substances, in the same manner as the rest of HSs [14,15]. The AD recalcitrance and partially soluble character of melanoidins might lead to problems in the AD-downstream processes, particularly during the treatment of reject water after digestate-dewatering [16,17].

During AD, nutrients are usually released from degraded substrates, thus the reject water contains elevated concentrations of total ammoniacal nitrogen (TAN) and PO_4^{3-}-P. In various WWTPs, TAN and PO_4^{3-}-P are removed before the reject water is recirculated to the WWTPs' headworks. In The Netherlands, several full-scale WWTPs apply struvite precipitation and subsequent partial nitritation/anammox (PN/A) to remove PO_4^{3-}-P and TAN [18–21].

Struvite precipitation is a chemical process in which Mg^{2+} reacts with PO_4^{3-}-P, water, and TAN to form a mineral, which precipitates, and can be separated from the liquid solution via sedimentation. The struvite stoichiometric reaction is shown in Eq. 1 [22]. Struvite precipitation is a two-step process until an equilibrium is reached: nucleation and crystal growth [23]. Nucleation is a first-order phase transition in which small embryos of a new solid phase are created in a large volume of the previous unstable phase [24]. Crystals growth is the step in which molecules aggregate to the previously created nuclei. The crystal growth step can also be accompanied by agglomeration, in which, small crystals merge to create bigger aggregates [25].

$$Mg^{2+} + NH_4^+ + H_nPO_4^{n-3} + 6H_2O \leftrightarrow MgNH_4PO_4 \bullet 6H_2O + nH^+ \quad n = [1,2,3] \tag{1}$$

The struvite precipitation process is pH dependent and requires strict control of the reactants, to ensure that the added amount of Mg^{2+} reacts with the PO_4^{3-}-P in solution. However, when it comes to struvite precipitation in reject water, TAN is generally not monitored since it is commonly in excess compared to PO_4^{3-}-P. The more-than-stoichiometric TAN concentration in reject water shifts the equilibrium towards the products formation, thereby enhancing precipitation (Eq. 1). The struvite precipitation process is currently commercially available at full-scale with brand names, such as Airprex® (Centrisys-CNP, USA), PHOSPAQ™ (Paques, Netherlands) and Pearl® (Ostara, Canada). The application of the struvite precipitation process in wastewater treatment provides a triple benefit: 1) it removes PO_4^{3-}-P and TAN from reject water, reducing the nutrient load in the mainstream treatment; 2) it reduces maintenance in the reject water pipelines and sludge dewatering equipment due to undesired precipitation and clogging; and 3) it produces a renewable slow-release fertiliser [26]. The use of struvite as fertiliser relies on its low solubility in water, which allows for a slow nutrient release, while it prevents leaching into underground water bodies [27].

The THP-AD recalcitrant HSs affect the struvite precipitation processes [28], although the exact mechanisms are yet not fully understood. Chemical properties inherent to the HSs, such as pH-dependent solubility and complexation properties, may interfere with the precipitation process and may affect the struvite characteristics. To the knowledge of the authors the literature addresses HSs as a set of compounds with similar characteristics and not considering the singularities among them. In our present work, we investigated the influence of HSs as melanoidins and humic acids on the struvite crystallisation process, evaluating the effects on the yields of nutrients precipitated, and the morphology of the crystals produced. The results were used to build a conceptual model which considers the influence of specific characteristics of HSs on the struvite precipitation process.

2. Materials and methods

2.1. Analytical measurements

The ultraviolet absorbance at 254 nm (UVA 254) and colour were measured using a UV–Vis spectrophotometer (Genesys 10S, Thermo Scientific, USA) in quartz and plastic cuvettes of 1 cm path length, respectively. Colour was measured at 475 nm using a 500 mg Pt-Co/L colour reference solution (Certipur® Merck, Germany). UVA 254 and colour measurements were expressed in 1/cm and mg Pt-Co/L, respectively. The concentrations of PO_4^{3-}-P, TAN, total organic carbon (TOC), and Mg^{2+} were determined using Hach Lange kits (Hach, Germany: LCK 350, LCK 303, LCK 386, and LCK 326, respectively). The spectrophotometer model DR3900 (Hach, Germany) was used to read the kits. Specific ultraviolet absorbance (SUVA) was calculated as the ratio of UVA 254 in 1/m to the concentration of TOC in mg/L (Edzwald and Van Benschoten 1990). Each sample was measured in triplicate, error bars are used to indicate the standard deviation of the measurements.

To evaluate the level of significance between the differences of the samples, single-factor ANOVA plus Tukey's HSD at 95 % confidence were used. Additionally, a two-tailed single sample *t*-test at 95 % confidence was used to compare experimental results with stoichiometric values.

2.2. Struvite precipitation tests

Struvite crystallisation tests were performed in triplicate using a 0.5 L Jar test device (VELP Scientifica, Italy), at a mixing speed of 160 rpm for one hour at 20 ± 1 °C, following the procedure described by Li, Huang, Boiarkina, Yu, Huang, Wang and Young [29]. The pH was measured online and manually controlled by adding 5 M NaOH. The volume of added NaOH was considered negligible, as it was <1 % of the total reaction volume. The term HSs refers to the melanoidins and humic acids used in our present study. The experimental design is shown in Table 1, where the samples were named after the concentration and type of HSs present, including: i) No-HSs, absence of HSs; ii)MEL-1, melanoidins 1 g TOC/L; iii) MEL-2, melanoidins 2 g TOC/L; iv) HA-1, humic acid 1 g TOC/L; i) HA-2, humic acid 2 g TOC/L. Table 2 shows humic acid and melanoidins stock solutions' preparation and characterisation. The reagents' concentrations in the crystallisation tests were 15 mM, 66.45 mM and 15 mM for Mg^{2+}, TAN and PO_4^{3-}-P, respectively. The nutrients and HSs concentrations were chosen to resemble typical values of reject water from WWTPs that aim for biological nutrient removal (BNR), having phosphate accumulating organisms in the waste activated sludge [30–35]. The reagents were added as $NaH_2PO_4{\cdot}H_2O$ (CAS: 10049-21-5, Sigma-Aldrich, Germany), NH_4Cl (CAS: 12125-02-9,

Table 1
Experimental design of crystallisation tests at different pH and HSs concentrations.

Run (triplicate)	pH	Melanoidins concentration g TOC/L	Humic acid concentration g TOC/L
1	6.50	0	0
2	7.25	0	0
3	8.00	0	0
4	6.50	1	0
5	7.25	1	0
6	8.00	1	0
7	6.50	2	0
8	7.25	2	0
9	8.00	2	0
10	6.50	0	1
11	7.25	0	1
12	8.00	0	1
13	6.50	0	2
14	7.25	0	2
15	8.00	0	2

Table 2
Characterisation of the stock solutions of HSs used in the experiments.

HSs stock solutions	UVA 254 (1/cm)	Colour (g Pt-Co/L)	TOC (g TOC/L	Preparation method
Melanoidins	605 ± 33	239 ± 33	24 ± 2	Autoclaving glucose 0.25 M, glycine 0.25 M, and $NaHCO_3$ 0.5 M at 121 °C for 3 h.
Humic acid	297 ± 17	183 ± 11	3.6 ± 0.2	Suspending 20 g/L of humic acid sodium salt in demineralised water.

Merck, Germany) and $MgCl_2$ (CAS: 7786-30-3, Sigma-Aldrich, Germany). After the crystallisation experiments, PO_4^{3-}-P and TAN were measured in the solution, and in the crystals formed. The soluble concentrations were measured directly using the Hach-Lange kits described in Section 2.1. The nutrients in the crystals were measured by dissolving 0.1 g of the precipitated solids in 5 mL of 1 M HNO_3 (Merck, Germany) [36], and then diluting the solution 100 times in demineralised water before measuring with the respective kits.

2.3. Solubility analysis of solubility of HSs at different pHs

HSs can be characterised based on their humic acid fraction (HAF) and fulvic acid fraction (FAF), which were measured as described by Klavins, Eglite and Serzane [37], using the method described by Zahmatkesh, Spanjers, Toran, Blánquez and van Lier [38]. The commercial humic acid used in our present study was obtained from humic acid sodium salt (CAS: 1415-93-6, Sigma-Aldrich, Germany), and a stock solution of melanoidins was prepared according to Dwyer, Starrenburg, Tait, Barr, Batstone and Lant [6]. A characterisation of the stock solutions is shown in Table 2. HAF and FAF in HSs, were measured by decreasing the pH to 2 using 5 M HCl, followed by separation of the precipitate using a Microspin 12 centrifuge (Biosan, Latvia) at 14,000 rpm (11,500 rcf) for 20 min. TOC was measured in both the original samples and the supernatant after acidification and centrifugation. In addition, solubility tests were performed at pH levels of 6.5, 7.25, and 8, corresponding to the pH levels used in the crystallisation experiments. The precipitated fraction was separated using the aforementioned methodology. Duplicate experiments were conducted, and the results are presented as the percentage of TOC that is soluble and particulate at the experiment pHs.

2.4. Microscopy and particle size distribution analysis (PSD)

Struvite samples produced during the crystallisation experiments were filtered through a 1.2 μm filter and dried to a constant weight in a vacuum desiccator at 20 ± 1 °C and −600 mbar. Digital Microscope (Keyence VHX-5000, Belgium) and an environmental scanning electron microscope (ESEM) model QUANTA FEG 650 (FEI, USA) were used to capture images of the produced struvite at different magnifications. The software of the digital microscope was utilized to measure the particle size distribution (PSD) of the crystals in the images, including the minimum and maximum Feret diameters. The aspect ratio was determined as the ratio of the maximum to minimum Feret diameters of each crystal. An aspect ratio of 1 means that the maximum and minimum Feret diameters are equal (perfect circle/sphere), and larger aspect ratios indicate elongated shapes. The results were plotted as “box and whisker” plots, with the boxes indicating the quartiles and the whiskers indicating the maximum and minimum values. The median and average were represented by a horizontal line in the middle and an “X”, respectively. Particles with a zero value for one of the Feret diameters in the images were excluded from the analysis and considered experimental errors.

2.5. Shear rate-induced breakage in struvite crystals

To investigate the effect of humic acid and melanoidins on struvite breakage, crystallisation experiments were performed under specific shear rates. A modular compact rheometer model MRC 302 (Anton Paar GmbH, Austria) was used to conduct the experiments. Struvite crystallisation tests were carried out in a measuring cup C-CC27/SS/AIR (Anton Paar GmbH, Austria) using a concentric cylinder CC27 (Anton Paar GmbH, Austria) at 20 °C. The volume of the 5 M NaOH solution, which was required to maintain the pH at 7.25 at the end of the reaction, was determined through preliminary experiments. The humic acid and melanoidins concentrations used in the experiments were the same as those in the struvite crystallisation experiments described in Section 2.2. The chosen shear rates for the experiments were 1-10-100-1000 1/s. The precipitates were analysed by measuring the minimum and maximum Feret diameters, and the aspect ratio was calculated using the method described in Section 2.4.

2.6. Complexation of reagents with HSs

Solutions of 15 mM of Mg^{2+} and PO_4^{3-}-P with 0, 1 and 2 g TOC/L (No-HSs, MEL-1, MEL-2, HA-1 and HA-2) were prepared and filtered in triplicate using nominal pore 1 kDa ultrafiltration membranes (Ultracel® regenerated cellulose, Merck Millipore, Germany) in a 50 mL AMICON® stirred cell (Merck Millipore, Germany). During filtration, 10 mL of permeate were collected and colour, UVA 254 and Mg^{2+} or PO_4^{3-}-P (depending on the assay) were measured. The results were expressed as the percentage of the fraction of ions of Mg^{2+} or PO_4^{3-}-P in the permeate over the initial concentration in the entire solution. The fraction that passed the ultrafiltration membrane over the initial concentration was called Mg^{2+} or PO_4^{3-}-P fraction in the permeate (Mg^{2+}-FP or PO_4^{3-}-P-FP, respectively).

3. Results and discussion

3.1. Characterisation of HSs solubility and results of complexation assays

The solubility of HSs and their complexes varies with the pH of the solution or suspension in which they are present [39,40]. Table 3 shows a solubility characterisation of the melanoidins and humic acid stock solutions used in our experiments. As shown in Table 3, melanoidins were completely soluble at all the pH values studied. Additionally, the melanoidins' structure contained 97 % FAF, which is soluble at any pH [37]. On the other hand, the humic acid stock solution was less soluble than the melanoidin solution, and its solubility slightly decreased at lower pH values used in the experiments. As anticipated for humic acid, the FAF only amounted to 6.4 % (soluble fraction at pH 2). SUVA results showed that the humic acids had a roughly three times higher degree of aromaticity than the melanoidins. In their study on natural freshwater, Kikuchi, Fujii, Terao, Jiwei, Lee and Yoshimura [41] found a positive

Table 3
Solubility and aromaticity characterisation of the HSs used in our present study at the studied pHs.

Characteristic	Melanoidins stock	Humic acid stock
Solubility at pH 6.5	Soluble: 100 ± 2 % TOC	87 ± 1 % TOC
Solubility at pH 7.25	Soluble: 100 ± 2 % TOC	89 ± 2 % TOC
Solubility at pH 8	Soluble: 100 ± 1 % TOC	91 ± 2 % TOC
Characterisation as HSs at pH 2 based on Klavins, Eglite and Serzane [37]	FAF: 97 ± 2 % TOC HAF: 3.4 ± 0.1 % TOC	FAF: 6.4 ± 0.3 % TOC HAF: 94 ± 4 % TOC
SUVA (L/m/mg TOC)	2.5 ± 0.2	8.0 ± 0.6

correlation between SUVA and metal complexation in the case of Fe and Cu. Therefore, it is reasonable to expect that humic acid complexes metals to a greater extent than melanoidins.

3.2. Complexation of HSs with Mg^{2+} and PO_4^{3-}-P

The complexation of cations with HSs depends on the presence and density of cation binding sites present in HSs moieties, which are mainly associated with hydroxyl, and carboxylic groups [42]. Fig. 1 shows the results of Mg^{2+} and PO_4^{3-}-P complexation assays performed at 1 and 2 g TOC/L of HSs. TAN was not tested because it was present in excess in the synthetic reject water. Expectedly, the complexation of PO_4^{3-}-P was not affected by the presence of melanoidins or humic acid at all pH levels studied, attributable to the negative charges of melanoidins, humic acid, and PO_4^{3-}-P repelling each other [43]. However, PO_4^{3-}-P can form binary complexes with HSs in the presence of multivalent cations such as Ca^{2+} [44]. Multivalent cation-mediated complexation was not tested in our study, but it is expected to occur in full-scale struvite precipitation installations, as AD reject water contains multiple multivalent cations [45]. Furthermore, in the assays without HSs only 92 % of PO_4^{3-}-P passed through the ultrafiltration membranes, while in the samples containing HSs, >95 % of the PO_4^{3-}-P reached the permeate. The observed differences were significant in all cases as shown by statistic tests (shown in the appendix, Table A1). The lower PO_4^{3-} —P concentration in the permeate likely can be attributed to the repulsion of the negatively charged regenerated cellulose ultrafiltration membrane [46] and the PO_4^{3-}-P anions. Nonetheless, and despite the abundant presence of negatively charged groups related to the melanoidins and humic acids in the solution, the available Na^+ ions present in HSs solutions may have partly neutralised the negative PO_4^{3-}-P charges, allowing membranes passage.

Conversely to PO_4^{3-}-P, Mg^{2+} was strongly complexed by HSs at all studied pH values (Fig. 1-b). Mg^{2+} complexation increased with the increased TOC concentration in both melanoidins and humic acid solutions. HSs-cation complexation varies with the specific characteristics of the HSs present [13,47,48]. Enhanced Mg^{2+} complexation may be associated with HSs aromaticity and the humic or fulvic acid character of the HSs used in our present study. Mantoura, Dickson and Riley [49] found that in general, fulvic acids complexed cations to a lower extent compared to humic acids. In our present study, the FAF in the purchased humic acid was substantially lower than in the experimentally produced melanoidins solution (Table 3). Additionally, the SUVA in humic acid was around three times higher than the SUVA of melanoidins (Table 3), suggesting higher aromaticity and complexing capacity in humic acid. The complexation of Mg^{2+} with HSs was not affected by pH, and the *p*-values in a single-factor ANOVA at 95 % confidence, comparing all used concentrations, were not statistically different, i.e., 0.51, 0.67, 0.99, 0.83, and 0.78 in the case of No-HSs, MEL-1, MEL-2, HA-1, and HA-2, respectively. This indifference to pH contradicts other studies that have found a clear correlation between pH and HSs complexation capacity [50,51]. However, our researched pH range of 6.5–8.0 was quite narrow and far from the theoretical neutralisation pH of HSs, which is around pH 3.0–4.5 [52]. The complexation of Mg^{2+} in reject water is of considerable importance for practice, since it would lower the degree of supersaturation of the struvite precipitation reaction (Eq. 1 and Eq. 2, respectively), and thus could hinder struvite formation.

Colour and UVA 254 were analysed to quantify the fraction of HSs that passed through a 1 kDa ultrafiltration membrane (shown in appendix Table A2 and A3). Around 15 % of the colour and 38 % of UVA 254 passed through the 1 kDa membrane in the case of MEL-1 and MEL-2, and 1 % and 3 % passed it in the case of HA-1 and HA-2, respectively. The lower fraction of colour and UVA 254 of humic acids in the 1 kDa permeate compared to melanoidins at the same concentrations, evidenced that the humic acid in the solution had higher MW.

3.3. Nutrients mass balances

Fig. 2 shows the levels of precipitated (P-) and soluble (S-) nutrients at the studied pH values and incremental concentrations of HSs. Our results indicated that an increase in pH led to an enhancement in struvite precipitation; molar ratios indeed confirmed the presence of struvite (Mg_{2+}:NH_4^+:PO_4^{3-} ≈ 1; appendix Fig. A1). The enhanced struvite formation at pH 7.25 and 8 is attributed to the higher degree of supersaturation induced by the elevated pH. For struvite, the degree of supersaturation (Ω) is defined in Eq. 2.

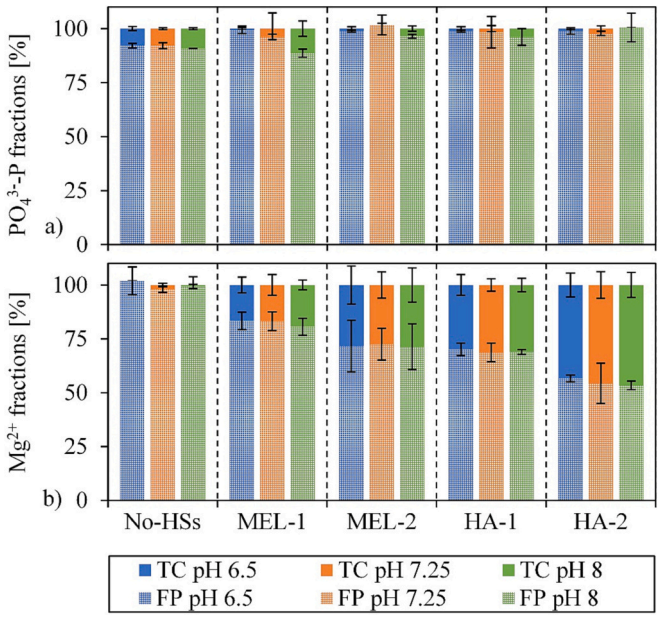

Fig. 1. Complexation experiments using PO_4^{3-}-P and Mg^{2+} with an incremental concentration of melanoidins and humic acid; a) PO_4^{3-}-P fractions; b) Mg^{2+} fractions. "TC" represents total concentration and "FP" represents the fraction in the permeates.

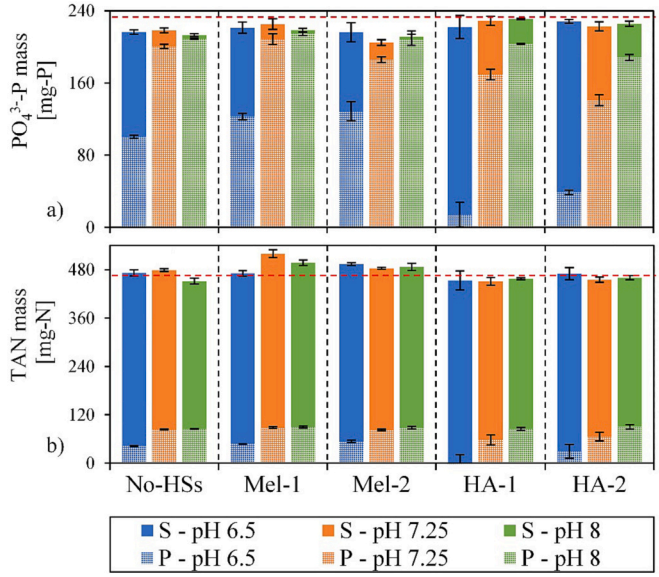

Fig. 2. Nutrients mass balances at different concentrations of melanoidins and humic acids at different pH values. a) PO_4^{3-}-P mass; b) TAN mass. "P" represents the nutrient mass in the precipitates, and "S" is the mass in the supernatants; the red-dashed lines represent the stoichiometric mass of nutrients. (For interpretation of the references to colour in this figure legend, the reader is referred to the web version of this article.)

$$\Omega = \sqrt[3]{\frac{a_1 \bullet \left[Mg^{2+}\right] a_2 \bullet \left[NH_4^+\right] a_3 \bullet \left[PO_4^{3-}\right]}{K_{sp}}} \quad (2)$$

where a_1, a_2, and a_3 represent the activity coefficients of Mg^{2+}, NH_4^+ and PO_4^{3-} and "[]" their molar concentrations, respectively; K_{sp} is the thermodynamic solubility product, which may vary between $4.37{\cdot}10^{-14}$ to $3.89{\cdot}10^{-10}$ depending on the method used for its determination [53]. Our results showed that variations in pH affected the speciation of reagents, which in turn affects Ω and the amount of produced struvite. Considering the speciation of the reagents in solution, Desmidt, Ghyselbrecht, Monballiu, Rabaey, Verstraete and Meesschaert [54] found that the optimum range for struvite precipitation is at pH 8–10; which is consistent with the lower precipitate yields at pH 6.5 found in our study. Barber [5] stated that the THP-AD-reject water tends to have a slight alkalic pH due to the elevated concentration of TAN, which may increase Ω, promoting uncontrolled struvite precipitation.

We also examined the effect of HSs on struvite precipitation. The presence of melanoidins at pH 7.25 and 8 did not significantly alter the fraction of TAN and PO_4^{3-}-P in the precipitates. However, at pH 6.5 the incremental melanoidins concentrations resulted in a higher percentage of PO_4^{3-}-P in the precipitates, from 43 % (No HSs) to 53 % and 55 % in the case of MEL-1 and MEL-2. The ANOVA test at 95 % confidence showed significant differences at pH 6.5 in the samples No-HSs, Mel-1 and Mel-2 samples (p-value = 0.0039), and Tukey HSD- test showed that the PO_4^{3-}-P measurements in MEL-1 and MEL-2 were equal (p-value = 0.53) and significantly higher than No-HSs (p-value = 0.013 and p-value = 0.004, respectively). At pH 6.5, MEL-1 and MEL-2 promoted struvite formation, presumably due to the addition of nucleation centres (seeding material), resulting from the partial solubility of melanoidins at lower pH values. Despite the high solubility of melanoidins (shown in Table) the impurities formed at decreased pH may act as seeding material and promote nucleation and further precipitation [55–58]. Likely, the formed impurities had a colloidal nature and thus remained in suspension during sample centrifugation for assessing the solubility.

In contrast to melanoidins, humic acid hindered struvite precipitation (Fig. 2) particularly at pH 6.5, in which only 6 % (HA-1) and 17 % (HA-2) of the PO_4^{3-}-P precipitated, compared to 43 % in No-HSs. Also at pH 7.25 and 8, the presence of humic acid reduced precipitation; however, this effect was much less than at the lowest pH tested. Previous studies also have reported inhibitory effects of humic substances on struvite precipitation. For instance, Zhou, Hu, Ren, Zhao, Jiang and Wang [59] found inhibition in struvite formation caused by 40 mg/L HSs, using HSs containing ≥90 % fulvic acid. Furthermore, Wei, Hong, Cui, Chen, Zhou, Zhao, Yin, Wang and Zhang [60] also found that humic acid caused inhibition of struvite nucleation and moderately hindered crystals growth; the study suggests that Mg^{2+} complexation in the humic acid matrix might have caused the inhibition. Complexation of HSs and Mg^{2+} has already been reported in literature [51,61]. Moreover, the experiments in our present work strongly suggested that HSs and particularly the humic acid – Mg^{2+} complexes, hindered struvite precipitation.

Finally, we assessed the mass balance of nutrients in each experiment and found that the discrepancy between supernatant plus precipitate was within 10 % of the initial nutrient mass (mean difference t-test at 95 % of confidence showed in Table A1 of appendix). Also, a single-factor ANOVA analysis at 95 % of confidence, showed that all summed masses deviated slightly (p-values of 1.52·10–4 and 3.28·10–9 in the case of PO_4^{3-}-P and TAN, respectively). The small differences are attributed to the heterogeneity of suspended samples and the interference of the PO_4^{3-}-P measurement with humic substances. TAN mass was found to be slightly higher than the expected value, possibly due to deamination of glycine in the melanoidins stock solution under high-temperature conditions. Deamination of proteins caused by exposure to high temperatures has been described before. Wilson and Novak [62] found ammonia production in thermal hydrolysis with bovine serum albumin already at 130 °C, which increased with the reaction temperature.

3.4. PSD and morphology of the produced crystals

The PSD and morphology of the produced crystals in the presence of melanoidins at different pH values are presented in Fig. 3. Crystals produced in presence of humic acid, could not be analysed, since humic acid precipitates clogged the filters, while the attached non-soluble humic particles influenced the crystal size (additional material, Fig. A2). Crystallisation experiments showed that in the absence of HSs (No-HSs), the size average and variability of crystals decreased with an increased pH. Minimum Feret diameters in No-HSs averaged 53 ± 36 μm, 50 ± 27 μm and 39 ± 18 μm at pH 6.5, 7.25 and 8 respectively; and maximum Feret diameters averaged 105 ± 68 μm, 94 ± 53 μm and 88 ± 43 μm at the same pH values, respectively. Increased pH resulted in smaller crystals, even though the mass balance showed a higher degree of TAN and PO_4^{3-}-P crystallisation under these conditions (Fig. 1). Supersaturation is described to be positively correlated with nucleation [58], and it defines the size of crystals [63]. In our present study, elevated pH induced elevated supersaturation indexes, which led to the formation of more nuclei producing more and smaller crystals. Shaddel, Ucar, Andreassen and Østerhus [63] described similar behaviour at pH 7.5, 8.5 and 9.5.

Furthermore, MEL-1 and MEL-2 solutions rendered smaller crystals compared to No-HSs, at all analysed pH values. However, the decrease in size with increasing pH was not consistent, and the largest crystals among MEL-1 were formed at pH 7.25, with average minimum and maximum Feret diameters of 39 μm and 61 μm, respectively. MEL-2 rendered decreased Feret diameters and higher size variability with increasing pH. The observed smaller Feret diameter of the formed crystals in presence of melanoidins, could jeopardize the separation of crystals and reject water in full scale struvite reactors. A low crystal diameter might lead to the need of different settling velocities in completely stirred systems or fluidised bed systems [64]. Also, small diameters are not efficient for secondary nucleation, which, according to Cayey and Estrin [65], only occurs with particles bigger than 220 μm,

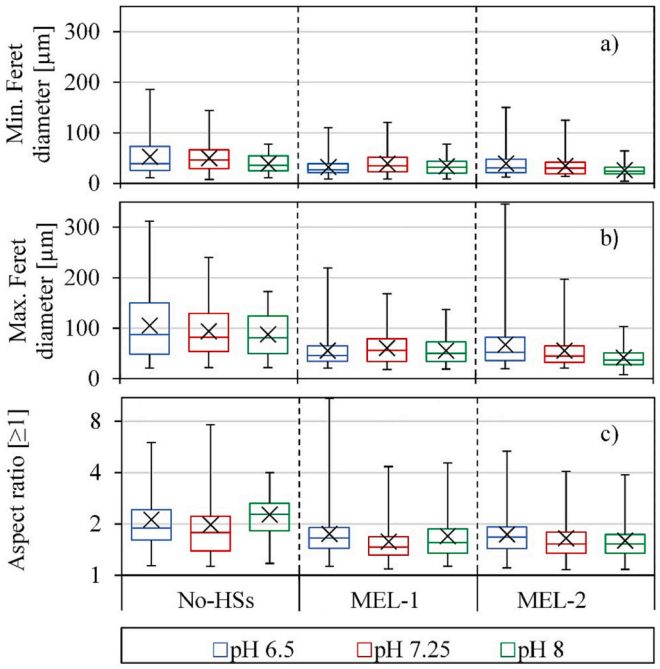

Fig. 3. PSD analysis of the crystallisation experiments: a) Minimum Feret diameter; b) Maximum Feret diameter; c) Aspect ratio (logarithmic scale). HSs data are not shown, since precipitates could not be determined.

due to their greater contact probabilities [66].

Crystal morphology was expressed by its aspect ratio (Fig. 3-c). The presence of melanoidins decreased the averaged aspect ratio regardless of the melanoidins concentration, compared with the No-HSs assays. The pH did not show a clear influence on the aspect ratio, except in MEL-2 where the crystals became less elongated with increased pH. Fig. 4 shows pictures of the crystals formed under the different conditions studied. No-HSs samples returned semi-transparent crystals with elongated blade-like shapes. These elongated shapes are in line with the observed aspect ratio data (Fig. 3-c). On the other hand, the addition of melanoidins, rendered more square-like shaped crystals with a distinctive brownish colour (Fig. 4), indicating the presence of melanoidins either at the surface or incorporated throughout the crystals, following the hypotheses of Zhou, Hu, Ren, Zhao, Jiang and Wang [59] and Abel-Denee, Abbott and Eskicioglu [67]. After nucleation, crystals-growth may occur following 2 processes, i) growing atom by atom, and ii) by aggregation of smaller crystals into bigger ones [25]. Melanoidins adsorbed on the struvite crystals during the growth process can be expected to interfere with both growth processes. This phenomenon was illustrated by the microscopic observations (Fig. 4); the presence of melanoidins led to brownish crystals. The same processes are proposed for other HSs, albeit, due to their lower solubility, the effects might be more pronounced. HSs might either act as a “glue” to aggregate the smaller particles into bigger ones (Fig. 6), or as a solid particle that hinders the aggregation process, decreasing the crystal size as described by Wei, Hong, Cui, Chen, Zhou, Zhao, Yin, Wang and Zhang [60]. The struvite growth process in presence of HSs is likely driven by the nature of the HSs and the crystals shear stress-induced breakage during the crystallisation process.

Fig. 5 shows a magnification of the crystals formed under the different applied conditions. In case of No-HSs, optic and ESEM microscopy showed that the increased pH caused so called “dendrites” formation in the crystal structure [68,69]. Dendrites are hierarchical structures, which grow far from the plane front in preferential direction, like a tree. Dendrites formation was observed in samples without HSs at elevated pH, likely due to the increased supersaturation index that produced more nuclei, from which the crystals grew from multiple sites [70]. Conversely, in the samples with melanoidins, optic microscopy showed homogenous pigmentation in struvite crystals, likely due to the high melanoidins' solubility (Fig. 5). In additional material, Fig. A2 shows humic acid precipitates using optical microscopy and ESEM. Humic acid formed a compact cake on the filters when the crystals were separated from the supernatant. The cake was characterised by a compact rigid structure and the cake particles differed distinctly from the crystals formed in the solution. ESEM revealed that the compact and rigid cake was likely formed due to adhesive forces between humic acid and the formed crystals. Optical microscopy clearly revealed the brown-coloured crystals and the tight interaction of particulate-humic material in the struvite crystals (Additional material, Fig. A2). The presence of HSs led to smaller-sized struvite crystals, but results could not reveal whether HSs hindered the crystals' growth or increased the crystals weakness, inducing breakage of the struvite formed.

3.5. Shear rate-induced breakage of the struvite produced

Experiments at increasing shear rate were conducted to further research the stability of the formed crystals. We assumed that the stability is inverse to the susceptibility of struvite crystals to break (breakage), which can be a combination of abrasion and cleavage. The breakage of formed crystals was indirectly measured by conducting struvite crystallisation experiments in the presence of melanoidins and humic acid at various shear rates ranging from 1, 10, 100, to 1000 1/s. The experiments were performed at pH 7.25. HA-2 was not analysed, because the produced precipitate remained adhered to the filters and yielded a low quantity. Figs. 6-a and b show the minimum and maximum Feret diameters of the formed struvite crystals at the different shear rates and HSs concentrations. The results showed that in the case of No-HSs, increased shear rate prevented the crystals to grow. No-HSs samples showed drastically reduced minimum and maximum Feret diameters, i.e., from 91 ± 108 μm to 8 ± 6 μm and 227 ± 207 to 22 ± 12 μm, respectively, with increased shear stress during crystal formation, from 1 to 1000 1/s. Also, the occurrence of big crystals (represented in Fig. 6 by upper whiskers) decreased, characterised by decreasing minimum and maximum Feret diameters from 742 to 13 μm and 1159 to 24 μm, at 1 and 1000 1/s, respectively. The aspect ratio of the crystals was not affected by the shear rate and crystal morphology remained mildly

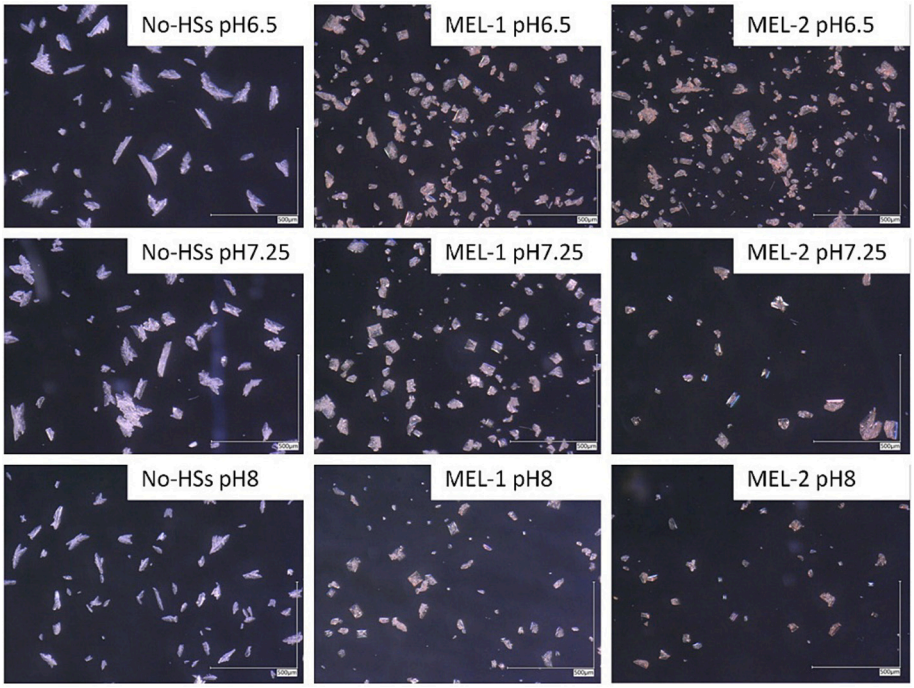

Fig. 4. Struvite pictures in presence of melanoidins at different pH conditions.

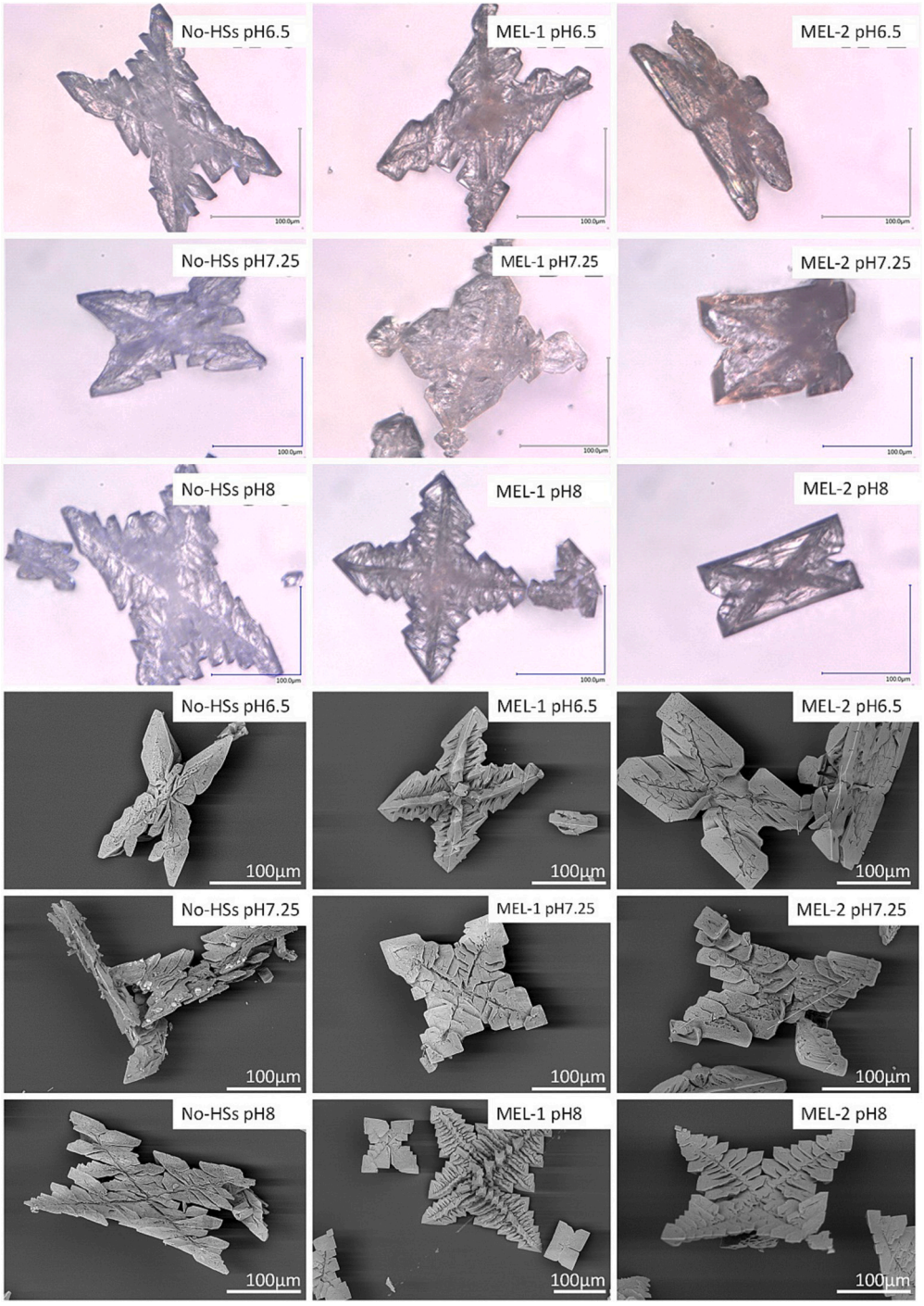

Fig. 5. Optic microscopy and ESEM pictures of specific crystals formed in the presence of melanoidins at different pH conditions.

elongated.

Melanoidins prevented breakage of the crystals, and possibly led to aggregation of particles that might have been broken without melanoidin addition. The minimum and maximum Feret diameters increased with the melanoidins concentration, particularly at 10 1/s, and decreased with shear rate. However, the size reduction induced by the increased shear stress was less prominent in MEL-1 and MEL-2 than in No-HSs, referring to both maximum and minimum Feret diameters. Melanoidins also decreased the aspect ratio at increased concentration, possibly due to breakage of needle-shaped particles and subsequent aggregation in non-preferential directions.

HA-1 showed the smallest particle size among the studied HSs samples. These small particles were probably a mixture of struvite and humic acid, as shown in Additional material Fig. A2. However, HA-1 did not show a clear trend regarding the size of maximum and minimum Feret diameters at shear rates of 10 and 100 1/s, while larger particles were formed at shear rates of 1 and 1000 1/s. The aspect ratio in HA-1 samples hardly changed with shear rate; nevertheless, the low values indicated the presence of rounded particles.

The observed results clearly showed that HSs addition increased the stability of the struvite crystals and rendered particles with a smaller aspect ratio. Compared to samples without HSs, the resulting particles with melanoidin addition had larger Feret diameters, whereas they were smaller with HAs addition. These results suggest that there are

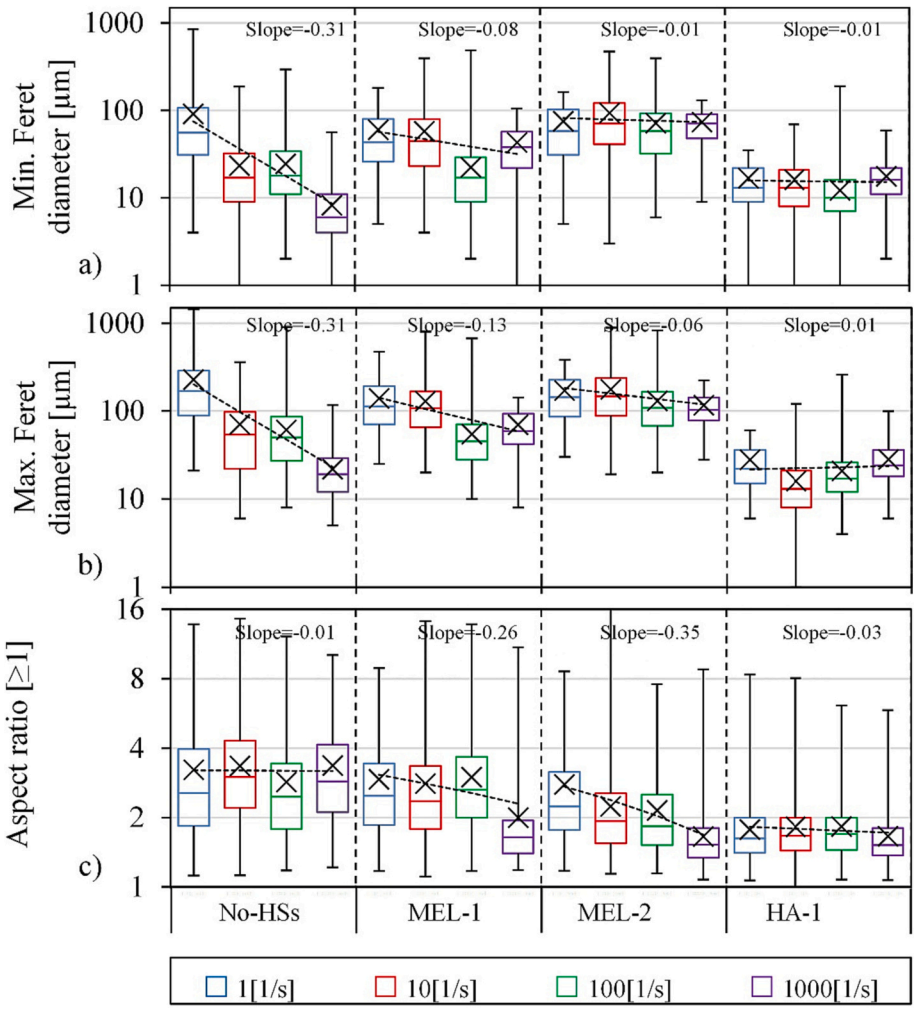

Fig. 6. Particle size distribution of struvite crystals in shear rate breakage tests at different HSs concentrations. a) Minimum Feret diameter (logarithmic scale); b) Maximum Feret diameter (logarithmic scale); c) Aspect ratio. The dotted lines represent a linear data fitting between the measured average values and the logarithm of the shear rate.

differences in the adhesive forces of melanoidins and HAs on struvite crystals causing different degrees of breakage. Such forces are most likely size and shape-dependent, as described by Carvill [71].

In the struvite-HSs interaction, two types of interactive forces play a prominent role. The struvite-struvite interactive forces have been described previously by Fromberg, Pawlik and Mavinic [72] as Van der Waals/electrostatic forces that are dependent on the distance between the crystals, as stated in the DLVO theory. In addition, the HSs-struvite forces are attributable to either adsorption as described by Zhang, Zhao, Ye and Xiao [73] and Wei, Hong, Cui, Chen, Zhou, Zhao, Yin, Wang and Zhang [60], or to DLVO-related forces, causing adsorption of the particulate/colloidal organic matter on, or in, the crystals. The latter is more apparent for humic acid containing a particulate fraction of 11 % (at pH 7.25), while melanoidins were fully soluble (Table). DLVO forces can be described by measuring zeta potential of the analysed suspensions, which is determined by the composition and ionic strength of the solution [72,74,75]. HSs have a negative zeta potential, however, Rodrigues, Brito, Janknecht, Proença and Nogueira [76] found that the presence of Mg^{2+} was able to elevate the zeta potential of HSs solutions at pH 4, 7, and 9 and created molecular aggregates. Besides, struvite zeta potential is predominantly negative and tends to decrease with increasing pH and Mg^{2+} concentration [72,77]. Considering that the zeta potentials of struvite and HSs are both negative, cations in solution (Mg^{2+} and NH_4^+), likely facilitated the formation of HSs-embedded crystals. Fig. 7 shows a schematic representation of the observed struvite crystal growth phenomena in the (non-) presence of HSs.

3.6. *Implications of THP-formed HSs on full-scale PO_4^{3-}-P removal*

The formation of HSs during THP through the Maillard reaction generates HSs with a wide range of molecular weights and solubilities [6,78], capable of forming complexes with cations in solution. Melanoidins present in the THP-reject water may complex Mg^{2+}, increasing the amount of Mg^{2+} salts required to achieve the desired Mg^{2+}/PO_4^{3-}-P molar ratio. Therefore, part of the PO_4^{3-}-P might not be removed due to Mg^{2+}-HSs chelation, or more Mg^{2+} salts may be needed to reach the desired concentration. Additionally, the colloidal or particulate fraction produced during THP may reach the struvite crystallisation reactors [5,16], leading to intercalation in the struvite crystals, affecting their sizes and settling times. HSs-intercalated struvite may compromise adoption of struvite as a fertiliser, because of the non-conventional colour of the crystals. Moreover, the adsorbed and/or embedded HSs on, or in, the struvite crystal might contain other cations, such as heavy metals [79–81], which might also compromise its use as fertiliser. The environmental implications of HSs and heavy metals in struvite is a subject of interest for further research. Furthermore, another observed consequence of THP pre-treatment is an increase in TAN concentration in anaerobic digesters [82,83]. The increase in TAN concentration during AD also increases the reactors' pH; this increase is commonly moderate since the anaerobic process occurs in a pH range suitable for

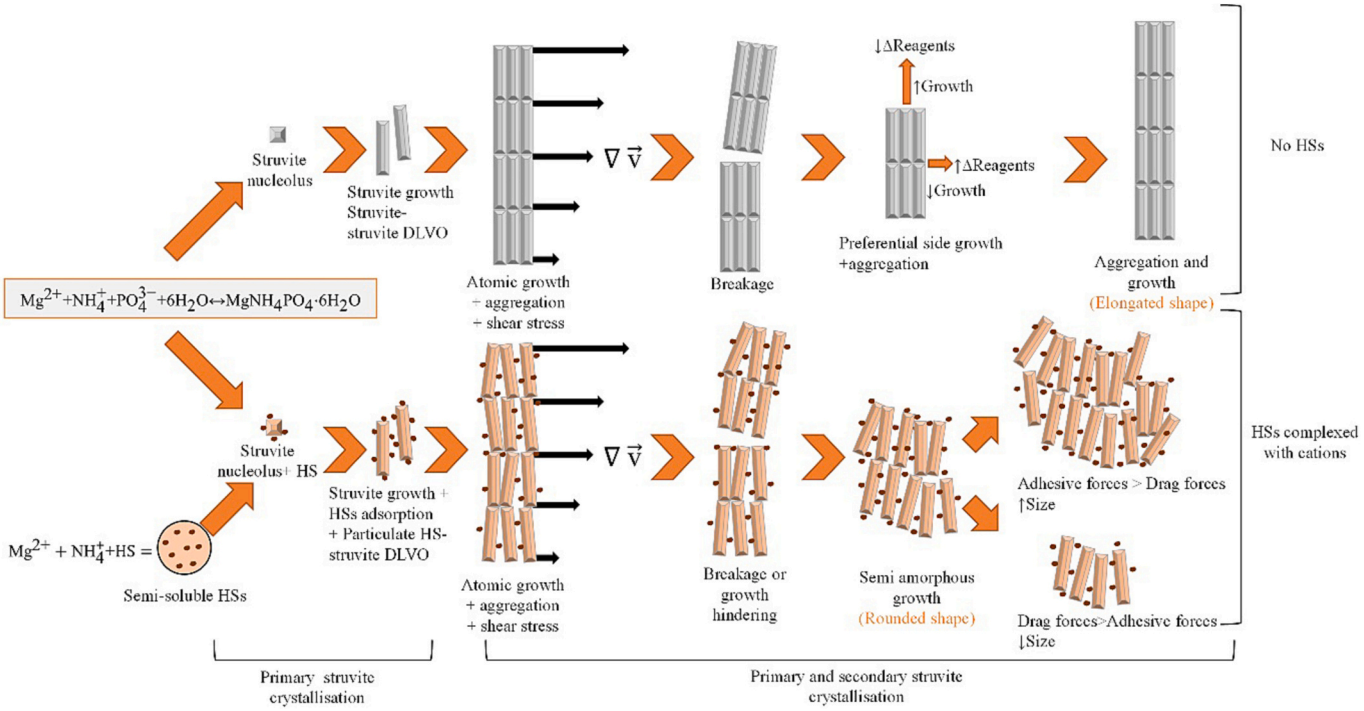

Fig. 7. Comparison between struvite crystal growth and breakage in the presence of melanoidins and humic acid (light brown coloured), and absence of HSs (grey coloured). The scheme indicates crystal growth, aggregation and breakage or growth hindering, HSs-crystal adsorption and intercalation, as well as the role of DLVO and adhesive forces. Shear forces are represented as the divergence of velocity ($\nabla\vec{v}$). (For interpretation of the references to colour in this figure legend, the reader is referred to the web version of this article.)

the microorganisms to grow (pH 7–8). The elevated TAN concentrations and the THP-induced pH increase might benefit struvite precipitation, since they both increase the supersaturation index and promote crystallisation.

4. Conclusions

Our present study led to the following conclusions:

- Melanoidins moderately, and humic acid strongly complexed Mg^{2+}. The complexing capacity of HSs is related to the HSs origin, particularly the soluble fraction of HSs, and its aromaticity.
- Humic acid strongly hindered struvite formation, likely due to Mg^{2+} complexation. The struvite crystallisation inhibition was higher at pH 6.5 compared to pH 7.25 and 8.
- Melanoidins presence decreased the maximum and minimum Feret diameters and the aspect ratio of the formed struvite crystal. In addition, melanoidins enhanced the stability of struvite crystals towards breakage at elevated shear rates, particularly when exceeding 10 1/s. Conversely, humic acid did not affect the struvite crystal stability towards abrasion or breakage and reduced the Feret diameters and aspect ratio.
- Adsorption of HSs on, or in, the produced struvite resulted in an evident change in colour.

Abbreviations

AD	anaerobic digestion
ESEM	environmental scanning electron microscope
FAF	fulvic acid fraction
HA-1	experiments in presence of humic substances as humic acids in a concentration of 1 g/L of total organic carbon
HA-2	experiments in presence of humic substances as humic acids in a concentration of 2 g/L of total organic carbon
HAF	humic acid fraction
HSs	humic substances
MEL-1	experiments in presence of humic substances as melanoidins in a concentration of 1 g/L of total organic carbon
MEL-2	experiments in presence of humic substances as melanoidins in a concentration of 2 g/L of total organic carbon
No-HSs	experiments without the presence of humic substances
PN/A	partial nitritation/anammox
PSD	particle size distribution
SUVA	specific ultraviolet absorbance
TAN	total ammoniacal nitrogen
THP	thermal hydrolysis process
TOC	total organic carbon
UVA 254	ultraviolet absorbance at 254 nm
WWTPs	wastewater treatment plants

CRediT authorship contribution statement

Javier Pavez-Jara: Conceptualization, Data curation, Formal analysis, Investigation, Methodology, Supervision, Validation, Visualization, Writing – original draft, Writing – review & editing. **Widya P. Iswarani:** Data curation, Investigation. **Jules B. van Lier:** Funding acquisition, Project administration, Resources, Supervision, Writing – review & editing. **Merle K. de Kreuk:** Funding acquisition, Project administration, Resources, Supervision, Writing – review & editing.

Declaration of generative AI and AI-assisted technologies in the writing process

During the preparation of this work the authors used ChatGPT-3.5 in order to improve readability. After using this tool/service, the authors reviewed and edited the content as needed and take full responsibility for the content of the publication.

Declaration of competing interest

The authors declare that they have no known competing financial interests or personal relationships that could have appeared to influence the work reported in this paper.

Data availability

Data will be made available on request.

Acknowledgements

This work was funded by ANID PFCHA/DOCEXT 72170548, TU Delft, STOWA, Paques BV, and Water Authorities from the Netherlands (Waterschap de Dommel, Waterschap Vechtstromen, Waterschap Vallei en Veluwe and Waterschap Limburg). This activity is co-financed by the Surcharge for Topconsortia for Knowledge and Innovation (TKI) of the Ministry of Economic Affairs, The Netherlands.

Appendix A. Supplementary data

Supplementary data to this article can be found online at https://doi.org/10.1016/j.jwpe.2024.104932.

References

[1] H. Carrere, C. Dumas, A. Battimelli, D.J. Batstone, J.P. Delgenes, J.P. Steyer, I. Ferrer, Pretreatment methods to improve sludge anaerobic degradability: a review, J. Hazard. Mater. 183 (1–3) (2010) 1–15, https://doi.org/10.1016/j.jhazmat.2010.06.129.

[2] L. Appels, J. Lauwers, J. Degrève, L. Helsen, B. Lievens, K. Willems, J. Van Impe, R. Dewil, Anaerobic digestion in global bio-energy production: potential and research challenges, Renew. Sust. Energ. Rev. 15 (9) (2011) 4295–4301, https://doi.org/10.1016/j.rser.2011.07.121.

[3] A.K. Sahu, I. Mitra, H. Kleiven, H.R. Holte, K. Svensson, Chapter 24 - Cambi Thermal Hydrolysis Process (CambiTHP) for sewage sludge treatment, in: A. An, V. Tyagi, M. Kumar, Z. Cetecioglu (Eds.), Clean Energy and Resource Recovery, Elsevier2022, pp. 405–422. doi:https://doi.org/10.1016/B978-0-323-90178-9.00020-2.

[4] P. Gahlot, G. Balasundaram, V.K. Tyagi, A.E. Atabani, S. Suthar, A.A. Kazmi, L. Štěpanec, D. Juchelková, A. Kumar, Principles and potential of thermal hydrolysis of sewage sludge to enhance anaerobic digestion, Environ. Res. 214 (2022) 113856, https://doi.org/10.1016/j.envres.2022.113856.

[5] W. Barber, Thermal hydrolysis for sewage treatment: a critical review, Water Res. 104 (2016) 53–71.

[6] J. Dwyer, D. Starrenburg, S. Tait, K. Barr, D.J. Batstone, P. Lant, Decreasing activated sludge thermal hydrolysis temperature reduces product colour, without decreasing degradability, Water Res. 42 (18) (2008) 4699–4709.

[7] L.V. Bork, P.T. Haase, S. Rohn, C. Kanzler, Structural characterization of polar melanoidins deriving from Maillard reaction intermediates – a model approach, Food Chem. 395 (2022) 133592, https://doi.org/10.1016/j.foodchem.2022.133592.

[8] G.P. Ellis, The Maillard reaction, in: M.L. Wolfrom (Ed.), Advances in Carbohydrate Chemistry, Academic Press 1959, pp. 63–134. doi:https://doi.org/10.1016/S0096-5332(08)60223-4.

[9] H.-Y. Wang, H. Qian, W.-R. Yao, Melanoidins produced by the Maillard reaction: structure and biological activity, Food Chem. 128 (3) (2011) 573–584, https://doi.org/10.1016/j.foodchem.2011.03.075.

[10] V.P. Migo, M. Matsumura, E.J. Del Rosario, H. Kataoka, The effect of pH and calcium ions on the destabilization of melanoidin, J. Ferment. Bioeng. 76 (1) (1993) 29–32, https://doi.org/10.1016/0922-338X(93)90048-D.

[11] K. Taguchi, Y. Sampei, The formation, and clay mineral and CaCO3 association reactions of melanoidins, Org. Geochem. 10 (4–6) (1986) 1081–1089.

[12] T. Gomyo, M. Horikoshi, On the interaction of melanoidin with metallic ions, Agric. Biol. Chem. 40 (1) (1976) 33–40, https://doi.org/10.1080/00021369.1976.10862003.

[13] J.A. Rufián-Henares, S.P. de la Cueva, Antimicrobial activity of coffee Melanoidins—a study of their metal-chelating properties, J. Agric. Food Chem. 57 (2) (2009) 432–438, https://doi.org/10.1021/jf8027842.

[14] E. Ortega-Martínez, R. Chamy, D. Jeison, Thermal pre-treatment: getting some insights on the formation of recalcitrant compounds and their effects on anaerobic digestion, J. Environ. Manag. 282 (2021) 111940, https://doi.org/10.1016/j.jenvman.2021.111940.

[15] S. Azman, A.F. Khadem, C.M. Plugge, A.J.M. Stams, S. Bec, G. Zeeman, Effect of humic acid on anaerobic digestion of cellulose and xylan in completely stirred tank reactors: inhibitory effect, mitigation of the inhibition and the dynamics of the microbial communities, Appl. Microbiol. Biotechnol. 101 (2) (2017) 889–901, https://doi.org/10.1007/s00253-016-8010-x.

[16] Q. Zhang, S.E. Vlaeminck, C. DeBarbadillo, C. Su, A. Al-Omari, B. Wett, T. Pümpel, A. Shaw, K. Chandran, S. Murthy, H. De Clippeleir, Supernatant organics from anaerobic digestion after thermal hydrolysis cause direct and/or diffusional activity loss for nitritation and anammox, Water Res. 143 (2018) 270–281, https://doi.org/10.1016/j.watres.2018.06.037.

[17] P.L. Ngo, I.A. Udugama, K.V. Gernaey, B.R. Young, S. Baroutian, Mechanisms, status, and challenges of thermal hydrolysis and advanced thermal hydrolysis processes in sewage sludge treatment, Chemosphere 281 (2021) 130890, https://doi.org/10.1016/j.chemosphere.2021.130890.

[18] W.R. Abma, W. Driessen, R. Haarhuis, M.C.M. van Loosdrecht, Upgrading of sewage treatment plant by sustainable and cost-effective separate treatment of industrial wastewater, Water Sci. Technol. 61 (7) (2010) 1715–1722, https://doi.org/10.2166/wst.2010.977.

[19] R. Taddeo, M. Honkanen, K. Kolppo, R. Lepistö, Nutrient management via struvite precipitation and recovery from various agroindustrial wastewaters: process feasibility and struvite quality, J. Environ. Manag. 212 (2018) 433–439, https://doi.org/10.1016/j.jenvman.2018.02.027.

[20] N. Marti, L. Pastor, A. Bouzas, J. Ferrer, A. Seco, Phosphorus recovery by struvite crystallization in WWTPs: influence of the sludge treatment line operation, Water Res. 44 (7) (2010) 2371–2379, https://doi.org/10.1016/j.watres.2009.12.043.

[21] S. Vlaeminck, H. De Clippeleir, W. Verstraete, Microbial resource management of one-stage partial nitritation/anammox, Microb. Biotechnol. 5 (3) (2012) 433–448.

[22] K.S. Le Corre, E. Valsami-Jones, P. Hobbs, S.A. Parsons, Phosphorus recovery from wastewater by struvite crystallization: a review, Crit. Rev. Environ. Sci. Technol. 39 (6) (2009) 433–477, https://doi.org/10.1080/10643380701640573.

[23] A.E. Nielsen, Nucleation and growth of crystals at high supersaturation, Krist. Tech. 4 (1) (1969) 17–38.

[24] J.J. De Yoreo, P.G. Vekilov, Principles of crystal nucleation and growth, Rev. Mineral. Geochem. 54 (1) (2003) 57–93, https://doi.org/10.2113/0540057.

[25] S.C. Galbraith, P.A. Schneider, A.E. Flood, Model-driven experimental evaluation of struvite nucleation, growth and aggregation kinetics, Water Res. 56 (2014) 122–132, https://doi.org/10.1016/j.watres.2014.03.002.

[26] L.E. de-Bashan, Y. Bashan, Recent advances in removing phosphorus from wastewater and its future use as fertilizer (1997–2003), Water Res. 38 (19) (2004) 4222–4246, https://doi.org/10.1016/j.watres.2004.07.014.

[27] E.V. Münch, K. Barr, Controlled struvite crystallisation for removing phosphorus from anaerobic digester sidestreams, Water Res. 35 (1) (2001) 151–159, https://doi.org/10.1016/S0043-1354(00)00236-0.

[28] M.T. Munir, B. Li, I. Boiarkina, S. Baroutian, W. Yu, B.R. Young, Phosphate recovery from hydrothermally treated sewage sludge using struvite precipitation, Bioresour. Technol. 239 (2017) 171–179, https://doi.org/10.1016/j.biortech.2017.04.129.

[29] B. Li, H.M. Huang, I. Boiarkina, W. Yu, Y.F. Huang, G.Q. Wang, B.R. Young, Phosphorus recovery through struvite crystallisation: recent developments in the understanding of operational factors, J. Environ. Manag. 248 (2019) 109254, https://doi.org/10.1016/j.jenvman.2019.07.025.

[30] J. De Vrieze, D. Smet, J. Klok, J. Colsen, L.T. Angenent, S.E. Vlaeminck, Thermophilic sludge digestion improves energy balance and nutrient recovery potential in full-scale municipal wastewater treatment plants, Bioresour. Technol. 218 (2016) 1237–1245, https://doi.org/10.1016/j.biortech.2016.06.119.

[31] B.J.C. Bergmans, A.M. Veltman, M.C.M. Van Loosdrecht, J.B. Van Lier, L. C. Rietveld, Struvite formation for enhanced dewaterability of digested wastewater sludge, Environ. Technol. 35 (5) (2014) 549–555, https://doi.org/10.1080/09593330.2013.837081.

[32] L. Pastor, N. Marti, A. Bouzas, A. Seco, Sewage sludge management for phosphorus recovery as struvite in EBPR wastewater treatment plants, Bioresour. Technol. 99 (11) (2008) 4817–4824, https://doi.org/10.1016/j.biortech.2007.09.054.

[33] X. Li, C. Liu, H. Xie, Y. Sun, S. Xu, G. Liu, Nitrogen removal of thermal hydrolysis-anaerobic digestion liquid: a review, Chemosphere 320 (2023) 138097, https://doi.org/10.1016/j.chemosphere.2023.138097.

[34] J.A. Pavez-Jara, J.B. van Lier, M.K. de Kreuk, Effects of thermal hydrolysis process-generated melanoidins on partial nitritation/anammox in full-scale installations treating waste activated sludge, J. Clean. Prod. 432 (2023), https://doi.org/10.1016/j.jclepro.2023.139767.

[35] A. Gupta, J.T. Novak, R. Zhao, Characterization of organic matter in the thermal hydrolysis pretreated anaerobic digestion return liquor, J. Environ. Chem. Eng. 3 (4, Part A) (2015) 2631–2636, https://doi.org/10.1016/j.jece.2015.07.029.

[36] J.C. Liu Warmadewanthi, Recovery of phosphate and ammonium as struvite from semiconductor wastewater, Sep. Purif. Technol. 64 (3) (2009) 368–373, https://doi.org/10.1016/j.seppur.2008.10.040.

[37] M. Klavins, L. Eglite, J. Serzane, Methods for analysis of aquatic humic substances, Crit. Rev. Anal. Chem. 29 (3) (1999) 187–193.

[38] M. Zahmatkesh, H. Spanjers, M.J. Toran, P. Blánquez, J.B. van Lier, Bioremoval of humic acid from water by white rot fungi: exploring the removal mechanisms, AMB Express 6 (1) (2016) 118, https://doi.org/10.1186/s13568-016-0293-x.

[39] J.M. Garcia-Mina, Stability, solubility and maximum metal binding capacity in metal–humic complexes involving humic substances extracted from peat and organic compost, Org. Geochem. 37 (12) (2006) 1960–1972, https://doi.org/10.1016/j.orggeochem.2006.07.027.

[40] E. Tipping, M. Ohnstad, Aggregation of aquatic humic substances, Chem. Geol. 44 (4) (1984) 349–357, https://doi.org/10.1016/0009-2541(84)90148-7.

[41] T. Kikuchi, M. Fujii, K. Terao, R. Jiwei, Y.P. Lee, C. Yoshimura, Correlations between aromaticity of dissolved organic matter and trace metal concentrations in natural and effluent waters: a case study in the Sagami River Basin, Japan, Sci. Total Environ. 576 (2017) 36–45, https://doi.org/10.1016/j.scitotenv.2016.10.068.

[42] F.J. Stevenson, Humus Chemistry: Genesis, Composition, Reactions, John Wiley & Sons, 1994.
[43] V.P. Migo, E.J. Del Rosario, M. Matsumura, Flocculation of melanoidins induced by inorganic ions, J. Ferment. Bioeng. 83 (3) (1997) 287–291, https://doi.org/10.1016/S0922-338X(97)80994-4.
[44] Y. Audette, D.S. Smith, C.T. Parsons, W. Chen, F. Rezanezhad, P. Van Cappellen, Phosphorus binding to soil organic matter via ternary complexes with calcium, Chemosphere 260 (2020) 127624, https://doi.org/10.1016/j.chemosphere.2020.127624.
[45] N.C. Ezebuiro, I. Körner, Characterisation of anaerobic digestion substrates regarding trace elements and determination of the influence of trace elements on the hydrolysis and acidification phases during the methanisation of a maize silage-based feedstock, J. Environ. Chem. Eng. 5 (1) (2017) 341–351, https://doi.org/10.1016/j.jece.2016.11.032.
[46] F. Weber, G. Koller, R. Schennach, I. Bernt, R. Eckhart, The surface charge of regenerated cellulose fibres, Cellulose 20 (6) (2013) 2719–2729, https://doi.org/10.1007/s10570-013-0047-8.
[47] F.J. Morales, C. Fernández-Fraguas, S. Jiménez-Pérez, Iron-binding ability of melanoidins from food and model systems, Food Chem. 90 (4) (2005) 821–827, https://doi.org/10.1016/j.foodchem.2004.05.030.
[48] M. Plavšić, B. Ćosović, C. Lee, Copper complexing properties of melanoidins and marine humic material, Sci. Total Environ. 366 (1) (2006) 310–319, https://doi.org/10.1016/j.scitotenv.2005.07.011.
[49] R. Mantoura, A. Dickson, J. Riley, The complexation of metals with humic materials in natural waters, Estuar. Coast. Mar. Sci. 6 (4) (1978) 387–408.
[50] M. Yan, Y. Lu, Y. Gao, M.F. Benedetti, G.V. Korshin, In-situ investigation of interactions between magnesium ion and natural organic matter, Environ. Sci. Technol. 49 (14) (2015) 8323–8329, https://doi.org/10.1021/acs.est.5b00003.
[51] G.O. Bosire, B.V. Kgarebe, J.C. Ngila, Experimental and theoretical characterization of metal complexation with humic acid, Anal. Lett. 49 (14) (2016) 2365–2376, https://doi.org/10.1080/00032719.2016.1141415.
[52] S. Karim, Y. Okuyama, M. Aoyama, Separation and characterization of the constituents of compost and soil humic acids by two-dimensional electrophoresis, Soil Sci. Plant Nutr. 59 (2) (2013) 130–141, https://doi.org/10.1080/00380768.2012.750230.
[53] M. Bhuiyan, D. Mavinic, R. Beckie, A solubility and thermodynamic study of struvite, Environ. Technol. 28 (9) (2007) 1015–1026.
[54] E. Desmidt, K. Ghyselbrecht, A. Monballiu, K. Rabaey, W. Verstraete, B. D. Meesschaert, Factors influencing urease driven struvite precipitation, Sep. Purif. Technol. 110 (2013) 150–157, https://doi.org/10.1016/j.seppur.2013.03.010.
[55] P. Battistoni, B. Paci, F. Fatone, P. Pavan, Phosphorus removal from supernatants at low concentration using packed and fluidized-bed reactors, Industrial & Engineering Chemistry Research 44(17) (2005) 6701–6707. doi:https://doi.org/10.1021/ie050186g.
[56] K.S. Le Corre, E. Valsami-Jones, P. Hobbs, B. Jefferson, S.A. Parsons, Struvite crystallisation and recovery using a stainless steel structure as a seed material, Water Res. 41 (11) (2007) 2449–2456, https://doi.org/10.1016/j.watres.2007.03.002.
[57] E. Ariyanto, T.K. Sen, H.M. Ang, The influence of various physico-chemical process parameters on kinetics and growth mechanism of struvite crystallisation, Adv. Powder Technol. 25 (2) (2014) 682–694, https://doi.org/10.1016/j.apt.2013.10.014.
[58] C.M. Mehta, D.J. Batstone, Nucleation and growth kinetics of struvite crystallization, Water Res. 47 (8) (2013) 2890–2900, https://doi.org/10.1016/j.watres.2013.03.007.
[59] Z. Zhou, D. Hu, W. Ren, Y. Zhao, L.-M. Jiang, L. Wang, Effect of humic substances on phosphorus removal by struvite precipitation, Chemosphere 141 (2015) 94–99, https://doi.org/10.1016/j.chemosphere.2015.06.089.
[60] L. Wei, T. Hong, K. Cui, T. Chen, Y. Zhou, Y. Zhao, Y. Yin, J. Wang, Q. Zhang, Probing the effect of humic acid on the nucleation and growth kinetics of struvite by constant composition technique, Chem. Eng. J. 378 (2019) 122130, https://doi.org/10.1016/j.cej.2019.122130.
[61] C. Zhao, C.Y. Tang, P. Li, P. Adrian, G. Hu, Perfluorooctane sulfonate removal by nanofiltration membrane—the effect and interaction of magnesium ion / humic acid, J. Membr. Sci. 503 (2016) 31–41, https://doi.org/10.1016/j.memsci.2015.12.049.
[62] C.A. Wilson, J.T. Novak, Hydrolysis of macromolecular components of primary and secondary wastewater sludge by thermal hydrolytic pretreatment, Water Res. 43 (18) (2009) 4489–4498, https://doi.org/10.1016/j.watres.2009.07.022.
[63] S. Shaddel, S. Ucar, J.-P. Andreassen, S.W. Østerhus, Engineering of struvite crystals by regulating supersaturation – correlation with phosphorus recovery, crystal morphology and process efficiency, J. Environ. Chem. Eng. 7 (1) (2019) 102918, https://doi.org/10.1016/j.jece.2019.102918.
[64] T.N. Vasa, S. Pothanamkandathil Chacko, Recovery of struvite from wastewaters as an eco-friendly fertilizer: review of the art and perspective for a sustainable agriculture practice in India, Sustainable Energy Technologies and Assessments 48 (2021) 101573, https://doi.org/10.1016/j.seta.2021.101573.
[65] N. Cayey, J. Estrin, Secondary nucleation in agitated, magnesium sulfate solutions, Ind. Eng. Chem. Fundam. 6 (1) (1967) 13–20.
[66] J.W. Mullin, Crystallization, Elsevier, 2001.
[67] M. Abel-Denee, T. Abbott, C. Eskicioglu, Using mass struvite precipitation to remove recalcitrant nutrients and micropollutants from anaerobic digestion dewatering centrate, Water Res. 132 (2018) 292–300, https://doi.org/10.1016/j.watres.2018.01.004.
[68] R. Kobayashi, Modeling and numerical simulations of dendritic crystal growth, Physica D: Nonlinear Phenomena 63 (3) (1993) 410–423, https://doi.org/10.1016/0167-2789(93)90120-P.
[69] D.N. Lee, Orientations of dendritic growth during solidification, Met. Mater. Int. 23 (2) (2017) 320–325, https://doi.org/10.1007/s12540-017-6360-2.
[70] M.E. Glicksman, A.O. Lupulescu, Dendritic crystal growth in pure materials, J. Cryst. Growth 264 (4) (2004) 541–549, https://doi.org/10.1016/j.jcrysgro.2003.12.034.
[71] J. Carvill, 4 - fluid mechanics, in: J. Carvill (Ed.), Mechanical Engineer's Data Handbook, Butterworth-Heinemann, Oxford, 1993, pp. 146–171, https://doi.org/10.1016/B978-0-08-051135-1.50009-1.
[72] M. Fromberg, M. Pawlik, D.S. Mavinic, Induction time and zeta potential study of nucleating and growing struvite crystals for phosphorus recovery improvements within fluidized bed reactors, Powder Technol. 360 (2020) 715–730, https://doi.org/10.1016/j.powtec.2019.09.067.
[73] Q. Zhang, S. Zhao, X. Ye, W. Xiao, Effects of organic substances on struvite crystallization and recovery, Desalin. Water Treat. 57 (23) (2016) 10924–10933, https://doi.org/10.1080/19443994.2015.1040850.
[74] Y. Zhang, K. Gu, K. Zhao, H. Deng, C. Hu, Enhancement of struvite generation and anti-fouling in an electro-AnMBR with Mg anode-MF membrane module, Water Res. 230 (2023) 119561, https://doi.org/10.1016/j.watres.2022.119561.
[75] S. Bhattacharjee, DLS and zeta potential – what they are and what they are not? J. Control. Release 235 (2016) 337–351, https://doi.org/10.1016/j.jconrel.2016.06.017.
[76] A. Rodrigues, A. Brito, P. Janknecht, M.F. Proença, R. Nogueira, Quantification of humic acids in surface water: effects of divalent cations, pH, and filtration, J. Environ. Monit. 11 (2) (2009) 377–382, https://doi.org/10.1039/B811942B.
[77] N.C. Bouropoulos, P.G. Koutsoukos, Spontaneous precipitation of struvite from aqueous solutions, J. Cryst. Growth 213 (3) (2000) 381–388, https://doi.org/10.1016/S0022-0248(00)00351-1.
[78] X. Liu, W. Wang, X. Gao, Y. Zhou, R. Shen, Effect of thermal pretreatment on the physical and chemical properties of municipal biomass waste, Waste Manag. 32 (2) (2012) 249–255, https://doi.org/10.1016/j.wasman.2011.09.027.
[79] S. Jansen, M. Paciolla, E. Ghabbour, G. Davies, J.M. Varnum, The role of metal complexation in the solubility and stability of humic acid, Mater. Sci. Eng. C 4 (3) (1996) 181–187, https://doi.org/10.1016/S0928-4931(96)00150-6.
[80] T.C.M. Yip, D.Y.S. Yan, M.M.T. Yui, D.C.W. Tsang, I.M.C. Lo, Heavy metal extraction from an artificially contaminated sandy soil under EDDS deficiency: significance of humic acid and chelant mixture, Chemosphere 80 (4) (2010) 416–421, https://doi.org/10.1016/j.chemosphere.2010.03.033.
[81] V. Bianchi, G. Masciandaro, D. Giraldi, B. Ceccanti, R. Iannelli, Enhanced heavy metal Phytoextraction from marine dredged sediments comparing conventional chelating agents (citric acid and EDTA) with humic substances, Water Air Soil Pollut. 193 (1–4) (2008) 323–333, https://doi.org/10.1007/s11270-008-9693-0.
[82] P. Ochs, B.D. Martin, E. Germain, T. Stephenson, M. van Loosdrecht, A. Soares, Ammonia removal from thermal hydrolysis dewatering liquors via three different deammonification technologies, Sci. Total Environ. 755 (2021) 142684, https://doi.org/10.1016/j.scitotenv.2020.142684.
[83] D. Jolis, High-solids anaerobic digestion of municipal sludge pretreated by thermal hydrolysis, Water Environ. Res. 80 (7) (2008) 654–662, https://doi.org/10.2175/193864708X267414.